

Imidotitanium Tris(pyrazolyl)hydroborates: Synthesis, Solution Dynamics, and Solid-State Structure

Simon C. Dunn, Philip Mountford,* and Oleg V. Shishkin

Department of Chemistry, University of Nottingham, Nottingham NG7 2RD, U.K.

Received August 11, 1995[⊗]

Reaction of $[\text{Ti}(\text{NBu}^t)\text{Cl}_2(\text{py-Bu}^t)_2]$ (**1**; $\text{py-Bu}^t = 4\text{-tert-butyl pyridine}$) with 1 equivalent of $\text{K}[\text{Tp}^{\text{Me}_2}]$, $\text{K}[\text{Tp}^{\text{Pri}}]$ or $\text{K}[\text{Tp}^{\text{Pri,Br}}]$ affords the corresponding complexes $[\text{Tp}^{\text{Me}_2}\text{Ti}(\text{NBu}^t)\text{Cl}(\text{py-Bu}^t)]$ (**2**), $[\text{Tp}^{\text{Pri}}\text{Ti}(\text{NBu}^t)\text{Cl}(\text{py-Bu}^t)]$ (**3**), and $[\text{Tp}^{\text{Pri,Br}}\text{Ti}(\text{NBu}^t)\text{Cl}(\text{py-Bu}^t)]$ (**4**), respectively, which are the first examples of imido Group 4 tris(pyrazolyl)hydroborates [$\text{Tp}^{\text{Me}_2} = \text{tris}(3,5\text{-dimethylpyrazolyl})\text{hydroborate}$; $\text{Tp}^{\text{Pri}} = \text{tris}(3\text{-isopropylpyrazolyl})\text{hydroborate}$; $\text{Tp}^{\text{Pri,Br}} = \text{tris}(3\text{-isopropyl-4-bromopyrazolyl})\text{hydroborate}$]. Complexes **2–4** are fluxional on the ^1H and ^{13}C NMR time scales, the spectra indicating restricted rotation about the Ti-py-Bu^t bond. Activation parameters for this dynamic process have been determined both by ^{13}C NMR lineshape analysis and by coalescence measurements. The solution-state structure for **2** has been unambiguously assigned from a low temperature, phase-sensitive ^1H NOESY DQF spectrum and the solid-state X-ray crystal structure of the dichloromethane solvate of **3** has been determined (space group $P2_1/n$; $a = 12.539(3)$, $b = 14.686(3)$, $c = 21.747(4)$ Å; $\beta = 91.28(3)^\circ$; $R_1 = 0.0694$ and $wR_2 = 0.154$ for 1578 observed reflections). ^{13}C NMR $\Delta\delta$ values ($\Delta\delta = \delta(\text{C}_\alpha) - \delta(\text{C}_\beta)$) for the *tert*-butyl imido ligand in **2–4** suggest that the donor ability of the tris(pyrazolyl)hydroborate ligands increases in the order $\text{Tp}^{\text{Pri,Br}} < \text{Tp}^{\text{Pri}} < \text{Tp}^{\text{Me}_2}$. None of these ligands, however, is as effective a donor to the metal center as either $\eta\text{-C}_5\text{H}_5$ or $\eta\text{-C}_5\text{Me}_5$.

Introduction

The study of transition metal imido complexes continues to be an area of intense activity,^{1,2} sustained, in part, by the capacity of such compounds to be valuable in organic transformations and catalysis.^{1–5} We have recently described a general route to sandwich and half-sandwich imidotitanium complexes starting from the readily-available precursor $[\text{Ti}(\text{NBu}^t)\text{Cl}_2(\text{py-Bu}^t)_2]$ (**1**; $\text{py-Bu}^t = 4\text{-tert-butyl pyridine}$)⁶ or its homologues.⁷ During the course of our studies we prepared some imido titanium tris(pyrazolyl)hydroborate complexes. Imido transition metal tris(pyrazolyl)hydroborates are, in general, rare^{8–10} and group 4 derivatives are completely unknown. This is in contrast to the well-developed oxo transition metal tris(pyrazolyl)hydroborate literature.^{11,12} We describe here the syntheses, solid- and solution-state structures, and solution dynamics of the first group 4 imido tris(pyrazolyl)hydroborates. Part of this work has been communicated previously.⁶

Experimental Section

General Methods and Instrumentation. All manipulations were carried out under an atmosphere of dinitrogen or argon using standard Schlenk-line or drybox techniques. All solvents were predried over

molecular sieves and refluxed over potassium (tetrahydrofuran, hexane) or calcium hydride (dichloromethane) under an atmosphere of dinitrogen and collected by distillation. CDCl_3 and CD_2Cl_2 were dried over calcium hydride, distilled under vacuum and stored under N_2 in Young's ampules. NMR samples were prepared in the drybox in teflon valve (Young's) tubes or sealed under vacuum at liquid nitrogen temperature.

^1H and ^{13}C NMR spectra were recorded on either a Bruker DRX 300, AM 400, or AMX 500 spectrometer. The spectra were referenced internally to residual protiosolvent (^1H) or solvent (^{13}C) resonances and are reported relative to tetramethylsilane ($\delta = 0$ ppm). Chemical shifts are quoted in δ (ppm) and coupling constants in Hz. IR spectra were recorded on a Nicolet 205 FTIR spectrometer in the range 4000–400 cm^{-1} . Samples were prepared in the dry box as Nujol mulls between CsI plates and all data are quoted in wavenumbers (cm^{-1}). Elemental analyses were carried out by the analysis department of this laboratory.

Preparations. $[\text{Ti}(\text{NBu}^t)\text{Cl}_2(\text{py-Bu}^t)_2]$ (**1**), $\text{K}[\text{Tp}^{\text{Me}_2}]$, $\text{K}[\text{Tp}^{\text{Pri}}]$, and $\text{K}[\text{Tp}^{\text{Pri,Br}}]$ were prepared according to literature methods.^{6,13,14}

(a) $[\text{Tp}^{\text{Me}_2}\text{Ti}(\text{NBu}^t)\text{Cl}(\text{py-Bu}^t)]$ (2**).** To a red solution of $[\text{Ti}(\text{NBu}^t)\text{Cl}_2(\text{py-Bu}^t)_2]$ (**1**, 1.0 g, 2.17 mmol) in THF (25 cm^3) at room temperature was added a solution of $\text{K}[\text{Tp}^{\text{Me}_2}]$ (0.730 g, 2.17 mmol) in THF (40 cm^3) over 5 min. The resultant cloudy, orange mixture was stirred for 12 h, the volatiles were removed under reduced pressure, and the residues were extracted into dichloromethane (20 cm^3) and filtered to remove KCl. The filtrate was reduced in volume to 15 cm^3 , carefully layered with hexane (60 cm^3), and then placed at -30°C for 3 d. Orange crystals of **2** formed, which were separated from the supernatant by decanting, washed with a dichloromethane–hexane mixture (1:4 by volume; 2×25 cm^3), and dried *in vacuo* whereupon they lost crystallinity. Yield: 0.700 g, 55%.

^1H NMR (CD_2Cl_2 , 223 K, 500 MHz): 9.74 (1 H, d, J 6.0 Hz, H_{od}), 7.55 (1 H, d, J 6.0 Hz, H_{md}), 7.28 (1 H, d, J 6.0 Hz, H_{ou}), 7.19 (1 H, d, J 6.0 Hz, H_{mu}), 5.90 (1 H, s, H_{42} or H_{43}), 5.88 (1 H, s, H_{43} or H_{42}), *ca.* 4.7 (1 H, br s, BH), 2.75 (3 H, s, Me_{d3}), 2.41 (3 H, s, Me_{u2}), 2.37 (3 H, s, Me_{u3}), 2.24 (3 H, s, Me_{u1}), 2.19 (3 H, s, Me_{d2}), 1.28 (9 H, s, $\text{NC}_5\text{H}_4\text{Bu}^t$), 1.16 (3 H, s, Me_{d1}), 1.10 (9 H, s, NBu^t). $^{13}\text{C}\{^1\text{H}\}$ NMR (CD_2Cl_2 , 223 K, 100.6 MHz): 162.9 (4- $\text{NC}_5\text{H}_4\text{Bu}^t$), 152.8 (C_{od} of py-Bu^t), 150.8, 150.1, 149.8 ($3 \times 3\text{-N}_2\text{C}_3\text{HMe}_2$), 148.3 (C_{ou} of py-Bu^t),

(13) Trofimenko, S.; Calabrese, J. C.; Domaille, P. J.; Thompson, J. S. *Inorg. Chem.* **1989**, 28, 1091.

(14) Trofimenko, S. *J. Am. Chem. Soc.* **1967**, 89, 3170 and 6288.

* Corresponding author. email: Philip.Mountford@Nottingham.ac.uk.

⊗ Abstract published in *Advance ACS Abstracts*, January 15, 1996.

- (1) Nugent, W. A.; Mayer, J. M. *Metal-Ligand Multiple Bonds*; Wiley-Interscience: New York, 1988.
- (2) Wigley, D. E. *Prog. Inorg. Chem.* **1994**, 42, 239.
- (3) Gibson, V. C. *Adv. Mater.* **1994**, 6, 37.
- (4) Coles, M. P.; Gibson, V. C. *Polym. Bull.* **1994**, 33, 529.
- (5) McGrane, P. L.; Livinghouse, T. *J. Am. Chem. Soc.* **1993**, 115, 11485.
- (6) Dunn, S. C.; Batsanov, A. S.; Mountford, P. *J. Chem. Soc., Chem. Commun.* **1994**, 2007.
- (7) Collier, P. E.; Dunn, S. C.; Mountford, P.; Nikonov, G. I.; Shishkin, O. V. Unpublished results.
- (8) Scheuer, S.; Fischer, J.; Kress, J. *Organometallics* **1995**, 14, 2627.
- (9) Sundermeyer, J.; Putterlik, J.; Foth, M.; Field, J. S.; Ramesar, N. *Chem. Ber.* **1994**, 127, 1201.
- (10) Powell, K. R.; Perez, P. J.; Luan, L.; Feng, S. G.; White, P. S.; Brookhart, M.; Templeton, J. L. *Organometallics* **1994**, 13, 1851.
- (11) Trofimenko, S. *Chem. Rev.* **1993**, 93, 943.
- (12) Trofimenko, S. *Prog. Inorg. Chem.* **1986**, 34, 115.

144.6, 144.4, 142.0 (3 × 5-N₂C₃HMe₂), 121.3 (*C_{mid}* of py-Bu⁴), 120.0 (*C_{mid}* of py-Bu³), 105.4, 105.3, 105.2 (3 × 4-N₂C₃HMe₂), 68.9 (NCMe₃), 34.9 (NC₅H₄CMe₃), 30.2 (NCMe₃), 29.8 (NC₅H₄CMe₃), 15.9, 15.5, 12.73, 12.71, 12.1, 11.6 (6 × N₂C₃HMe₂). Ir: ν(B-H) 2549 cm⁻¹. Anal. Calcd for C₂₈H₄₄BClN₈Ti: C, 57.3; H, 7.6; N, 19.1. Found: C, 57.2; H, 7.7; N, 19.6.

(b) [Tp^{Pri}Ti(NBu⁴)Cl(py-Bu⁴)] (3). To a red solution of [Ti(NBu⁴)Cl₂(py-Bu⁴)₂] (1, 1.0g, 2.17 mmol) in THF (25 cm³) at room temperature was added a solution of K[Tp^{Pri}] (0.822 g, 2.17 mmol) in THF (40 cm³) over 5 min. The resultant cloudy, orange mixture was stirred for 12 h, the volatiles were removed under reduced pressure, and the residues were extracted into dichloromethane (15 cm³) and filtered to remove KCl. The filtrate was reduced in volume to 15 cm³, carefully layered with hexane (75 cm³), and then placed at -30 °C for 3 d. Orange crystals formed, which were separated from the supernatant by decanting, washed with a dichloromethane-hexane mixture (1:5 by volume; 2 × 25 cm³), and dried *in vacuo* to give 3 as a dichloromethane solvate. Yield: 0.931 g, 68%. These crystals were suitable for an X-ray structure determination (*vide infra*).

¹H NMR (CD₂Cl₂, 218 K, 400 MHz): 9.75 (1 H, br d, *J* 6.0, *H_{od}*), 7.99 (1 H, br s, 5-N₂C₃PrⁱH₂), 7.74 (2 H, overlapping 2 × br m, 5-N₂C₃PrⁱH₂ and *H_{mid}*), 7.39 (1 H, br s, 5-N₂C₃PrⁱH₂), 7.19 (2 H, overlapping 2 × br m, *H_{ou}* and *H_{mid}*), 6.19 (2 H, overlapping 2 × br m, 2 × 4-N₂C₃PrⁱH₂), 5.78 (1 H, br m, 4-N₂C₃PrⁱH₂), 4.26 (2 H, overlapping br s and br sept, *J* ca. 7 Hz, *BH* and *CHMe₂*), 3.53, 2.07 (2 × 1 H, 2 × br sept, *J* ca. 7 Hz, 2 × *CHMe₂*), 1.35–1.20 (18 H, overlapping 3 × br d and s, *J* ca. 7 Hz, 3 × *CHMe₂* and NC₅H₄Bu^t), 1.15 (9 H, s, NBu^t), 0.91, 0.72, 0.29 (3 × 3H, 3 × br d, *J* ca. 7 Hz, 3 × *CHMe₂*). ¹³C{¹H} NMR (CD₂Cl₂, 218 K, 100.6 MHz): 163.5, 163.2, 163.1, 162.8 (3 × 3-N₂C₃PrⁱH₂ and 4-NC₅H₄Bu^t), 153.1 (*C_{od}* of py-Bu⁴), 149.8 (*C_{ou}* of py-Bu⁴), 137.1, 136.9, 134.7 (3 × 5-N₂C₃PrⁱH₂), 121.9 (*C_{mid}* of py-Bu⁴), 120.8 (*C_{mid}* of py-Bu³), 101.3, 100.9, 100.8 (3 × 4-N₂C₃PrⁱH₂), 70.1 (NCMe₃), 35.2 (NC₅H₄CMe₃), 30.3 (NCMe₃), 29.9 (NC₅H₄CMe₃), 27.6, 27.2, 26.7 (3 × *CHMe₂*), 25.5, 24.5, 23.8 (two signals overlapping), 22.9, 22.0 (6 × *CHMe₂*). Ir: ν(B-H) 2440 and 2460 cm⁻¹ (two bands due to site splitting). Anal. Calcd for C_{31.5}H₅₁BCl₂N₈Ti: C, 56.3; H, 7.7; N, 16.7. Found: C, 55.2; H, 7.9; N, 16.2.

(c) [Tp^{Pri,Br}Ti(NBu⁴)Cl(py-Bu⁴)] (4). To a red solution of [Ti(NBu⁴)Cl₂(py-Bu⁴)₂] (1, 1.0 g, 2.17 mmol) in THF (25 cm³) at room temperature was added a solution of K[Tp^{Pri,Br}] (1.336 g, 2.17 mmol) in THF (40 cm³) over 5 min. The resultant cloudy, orange mixture was stirred for 12 h, the volatiles were removed under reduced pressure, and the residues were extracted into dichloromethane (15 cm³) and filtered to remove KCl. The filtrate was reduced in volume to 15 cm³, carefully layered with hexane (75 cm³) and then placed at -30 °C for 3 d. Orange microcrystals formed which were separated from the supernatant by decanting, washed with a dichloromethane-hexane mixture (1:5 by volume; 2 × 25 cm³) and dried *in vacuo* to give 4 as a dichloromethane solvate. Yield: 0.531 g, 28%.

¹H NMR (CD₂Cl₂, 218 K, 400 MHz): 9.66 (1 H, br d, *J* 5.8, *H_{od}*), 7.79 (1 H, s, 5-N₂C₃PrⁱBrH), 7.67 (2 H, overlapping s and d, *J* 5.8 Hz, 5-N₂C₃PrⁱBrH and *H_{mid}*), 7.44 (1 H, s, 5-N₂C₃PrⁱBrH), 7.24 (2 H, s, overlapping *H_{ou}* and *H_{mid}*), 4.43 (1 H, sept, *J* 7.2 Hz, *CHMe₂*), 4.18 (1 H, br s, *BH*), 3.87, 2.37 (2 × 1 H, 2 × sept, *J* 7.2 Hz, 2 × *CHMe₂*), 1.45–1.30 (2 × 3 H, overlapping 2 × d, *J* 7.2 Hz, 2 × *CHMe₂*), 1.29 (3 H, d, *J* 7.2 Hz, *CHMe₂*), 1.25 (9 H, s, NC₅H₄Bu^t), 1.13 (9 H, s, NBu^t), 1.05, 0.84, 0.37 (3 × 3 H, 3 × d, *J* 7.2 Hz, 3 × *CHMe₂*). ¹³C{¹H} NMR (CD₂Cl₂, 218 K, 100.6 MHz): 163.7 (4-NC₅H₄Bu^t), 157.4, 157.1, 156.5 (3 × 3-N₂C₃PrⁱBrH), 152.9 (*C_{od}* of py-Bu⁴), 149.7 (*C_{ou}* of py-Bu⁴), 138.7, 138.0, 136.2 (3 × 5-N₂C₃PrⁱBrH), 122.4 (*C_{mid}* of py-Bu⁴), 121.1 (*C_{mid}* of py-Bu³), 91.1, 90.8, 90.4 (3 × 4-N₂C₃PrⁱBrH), 71.1 (NCMe₃), 35.2 (NC₅H₄CMe₃), 30.1 (NCMe₃), 29.9 (NC₅H₄CMe₃), 28.3, 27.8, 27.2 (3 × *CHMe₂*), 21.2, 20.6, 20.1, 19.4, 18.9, 18.1 (6 × *CHMe₂*). Ir: ν(B-H) 2452 cm⁻¹. Anal. Calcd for C_{31.5}H₄₈BBr₃Cl₂N₈Ti: C, 41.7; H, 5.3; N, 12.3. Found: C, 41.8; H, 5.9; N, 12.0.

Crystal Structure Determination. Crystals of a dichloromethane solvate (half-occupancy in the asymmetric unit) of [Tp^{Pri}Ti(NBu⁴)Cl(py-Bu⁴)] (3) were grown by layering a dichloromethane solution of 3 with hexane and cooling the mixture to -30 °C for 3 days. Data collection and processing parameters are listed in Table 1 and selected bond lengths and angles are in Table 2. A crystal of 3 was sealed in

Table 1. Crystal data for [Tp^{Pri}Ti(NBu⁴)Cl(py-Bu⁴)]·0.5(CH₂Cl₂) [3·0.5(CH₂Cl₂)]

empirical formula:	C _{31.5} H ₅₁ BCl ₂ N ₈ Ti
fw =	671.41
temperature =	293(2) K
wavelength =	0.71073 Å
crystal syst:	monoclinic
space group:	<i>P</i> 2 ₁ / <i>n</i>
unit cell dimens:	<i>a</i> = 12.539(3) Å, <i>c</i> = 21.747(4) Å,
	<i>b</i> = 14.686(3) Å, β = 91.28(3)°
volume =	4004(2) Å ³
<i>Z</i> =	4
density (calculated) =	1.114 g cm ⁻³
abs coeff =	0.377 mm ⁻¹
<i>F</i> (000) =	1428
cryst size =	0.40 × 0.20 × 0.20 mm
θ _{min} /θ _{max} =	1.67/22.95°
index ranges:	0 ≤ <i>h</i> ≤ 13, 0 ≤ <i>k</i> ≤ 16, -23 ≤ <i>l</i> ≤ +23
no. of reflns colld:	5719
no. of indep reflns:	5427 [R(int) = 0.0614]
refinement method:	full-matrix least-squares on <i>F</i> ²
data/restraints/params:	5372/0/329
goodness-of-fit:	0.782
final <i>R</i> indices [F > 4σ(<i>F</i>)]:	<i>R</i> ₁ ^a = 0.0694, <i>wR</i> ₂ ^b = 0.1545
<i>R</i> indices (all data):	<i>R</i> ₁ = 0.3250, <i>wR</i> ₂ = 0.3032
extinction coeff:	0.0114(12)
largest diff peak and hole:	+0.579 and -0.463 e Å ⁻³

^a *R*₁ = Σ||*F*_o| - |*F*_c||/Σ|*F*_o|. ^b *wR*₂ = [Σ[w(*F*_o² - *F*_c²)²]/Σ[w(*F*_o²)]^{1/2}.
^c Goodness of fit = [Σ[w(*F*_o² - *F*_c²)²]/(N_{observns} - N_{params})^{1/2}; based on all data.

Table 2. Selected Bond Lengths (Å) and Angles (deg) for [Tp^{Pri}Ti(NBu⁴)Cl(py-Bu⁴)] (3)

Ti(1)–N(1)	1.708(6)	N(5)–Ti(1)–N(2)	160.3(2)
Ti(1)–N(2)	2.221(6)	N(7)–Ti(1)–N(2)	87.6(2)
Ti(1)–N(3)	2.417(6)	N(1)–Ti(1)–Cl(1)	94.0(2)
Ti(1)–N(5)	2.176(7)	N(5)–Ti(1)–Cl(1)	91.9(2)
Ti(1)–N(7)	2.208(6)	N(7)–Ti(1)–Cl(1)	163.9(2)
Ti(1)–Cl(1)	2.392(3)	N(2)–Ti(1)–Cl(1)	95.8(2)
B(1)–N(4)	1.485(11)	N(1)–Ti(1)–N(3)	170.4(3)
B(1)–N(6)	1.532(11)	N(5)–Ti(1)–N(3)	84.3(2)
B(1)–N(8)	1.528(11)	N(7)–Ti(1)–N(3)	82.7(2)
N(1)–Ti(1)–N(5)	104.8(3)	Cl(1)–Ti(1)–N(3)	82.5(2)
N(1)–Ti(1)–N(7)	101.6(3)	N(4)–B(1)–N(8)	110.1(7)
N(5)–Ti(1)–N(7)	80.3(2)	N(4)–B(1)–N(6)	110.6(7)
N(1)–Ti(1)–N(2)	92.8(3)	N(8)–B(1)–N(6)	108.4(7)
N(2)–Ti(1)–N(3)	78.8(2)	C(1)–N(1)–Ti(1)	169.1(6)

a Lindemann glass capillary under N₂ and transferred to the goniometer head of an Enraf-Nonius CAD4 diffractometer. Unit cell parameters were calculated from the setting angles of 25 reflections. Reflections were measured in the ω–2θ scan mode. The data were corrected for Lorentz and polarization effects, equivalent reflections were merged, and systematically absent reflections were rejected. The Ti and Cl atom positions were located from a Patterson synthesis. Subsequent difference Fourier syntheses revealed the positions of all other non-hydrogen atoms, including a dichloromethane solvent molecule which was refined with an occupancy factor of 0.5 (as confirmed by the ¹H NMR spectrum of a sample of the crystals in CDCl₃ and also by an elemental analysis). Non-hydrogen atoms were refined against all *F*_o² with anisotropic displacement parameters by full-matrix least-squares procedures with the exception of B(1), N(4), N(6), N(8), the ring carbons of the pyrazolyl rings and the ring carbons of the *tert*-butyl pyridine ring which were refined in the isotropic approximation due to a lack of observed data [1578 reflections had *F*_o > 4σ(*F*_o) giving an “observed” data:parameter ratio of 4.8:1]. Hydrogen atoms were placed in estimated positions [C–H = 0.98 (bonded to tertiary carbon), 0.96 (methyl groups), 0.93 (aromatic rings) Å; B–H = 1.10 Å] with fixed isotropic displacement parameters [1.5 (methyl groups) or 1.2 (others) × the isotropic, or equivalent isotropic, temperature factor of the carbon atom to which they were bonded] and refined “riding” on their supporting carbon atoms. Methyl groups were allowed to rotate. A standard weighting scheme was applied and the data were corrected for the effects of anomalous dispersion and isotropic extinction in the final stages of

refinement. All crystallographic calculations were performed using the SHELX-86 and SHELXL-93 programs.^{15,16}

The methyl carbons of the py-Bu^t *tert*-butyl group gave relatively large equivalent isotropic displacement parameters (see Supporting Information). Attempts to define a fractionally disordered model for this Bu^t group were unsuccessful and it was treated as fully ordered. The relatively large equivalent isotropic displacement parameters for the C and Cl atoms of the fractional occupancy CH₂Cl₂ molecule may reflect unresolved disorder or, since displacement parameters and occupancy factors are correlated, a slightly lower true value for the fractional occupancy than that actually used (0.5). The choice of 0.5 for the occupancy of the CH₂Cl₂ molecule was based on an ¹H NMR spectrum and elemental analysis of some of the crystals, and there is no justification for choosing a different occupancy factor.

Results and Discussion

Syntheses. Our initial attempts to prepare imidotitanium tris(3,5-dimethylpyrazolyl)hydroborate derivatives employed methods designed to introduce an alkylimido or -amide functionality onto a preformed {Tp^{Me2}Ti} fragment starting from [Tp^{Me2}-TiCl₃].¹⁷ This strategy is analogous to that used recently by Roesky and co-workers in the synthesis of η -cyclopentadienyl (*tert*-butylamido)- and -(*tert*-butylimido)titanium complexes from η -cyclopentadienyltitanium trichloride precursors.¹⁸ However, we have found that treatment of [Tp^{Me2}TiCl₃] with Bu^t-NH₂, Li[Bu^tNH], or MeN(SiMe₃)₂ under a variety of conditions led either to reduction to uncharacterized Ti^{III} products or to no reaction occurring at all. We note that reaction of [Tp^{Me2}-TiCl₃] with Me₂NNMeH at room temperature produces the Ti^{III} product [NHMe₂NHMe]⁺[Tp^{Me2}Ti^(III)Cl₃]⁻, while [Tp^{Me2}TiCl₂(3,5-dimethylpyrazole)] is the product if this reaction is carried out in refluxing THF.¹⁹ Attempted preparation of zirconium tris(3,5-dimethylpyrazolyl)hydroborato zirconium amides from [Tp^{Me2}ZrCl₃] and either Li[Et₂N] or Li[PhNH] also fails, giving consumption of starting material but no tractable product.²⁰

Since direct introduction of amido or imido functional groups into [Tp^{Me2}TiCl₃] was unsuccessful, we sought another synthetic route. Reaction of THF solutions of the *tert*-butylimido complex [Ti(NBu^t)Cl₂(py-Bu^t)₂]⁶ (**1**) with potassium salts of the desired tris(substituted-pyrazolyl)hydroborate, specifically K[Tp^{Me2}], K[Tp^{Pri}], or K[Tp^{Pri,Br}], affords the corresponding complexes [Tp^{Me2}Ti(NBu^t)Cl(py-Bu^t)]² (**2**), [Tp^{Pri}Ti(NBu^t)Cl(py-Bu^t)]³ (**3**), and [Tp^{Pri,Br}Ti(NBu^t)Cl(py-Bu^t)]⁴ respectively in 28–68% isolated yield [Scheme 1; Tp^{Pri} = tris(3-isopropylpyrazolyl)-hydroborate; Tp^{Pri,Br} = tris(3-isopropyl-4-bromopyrazolyl)-hydroborate]. The new compounds **2–4** are orange in color and are air- and water-sensitive in solution, rapidly forming a white, insoluble precipitate. They have been characterized by ¹H and ¹³C NMR and IR spectroscopy, elemental analysis, and (for **3**) X-ray diffraction (*vide infra*).

The smooth synthesis of **2–4** from [Ti(NBu^t)Cl₂(py-Bu^t)₂] may, in part, be attributed to the strong π -donor ability of the *tert*-butylimido ligand,^{1,2} which should make the titanium center in [Ti(NBu^t)Cl₂(py-Bu^t)₂] more difficult to reduce. This hypothesis agrees well with our other recent observations that a range of anionic and dianionic ligands will substitute one or both Cl and py-Bu^t ligands in [Ti(NBu^t)Cl₂(py-Bu^t)₂] without any redox side reactions.⁶ It is important in the reactions

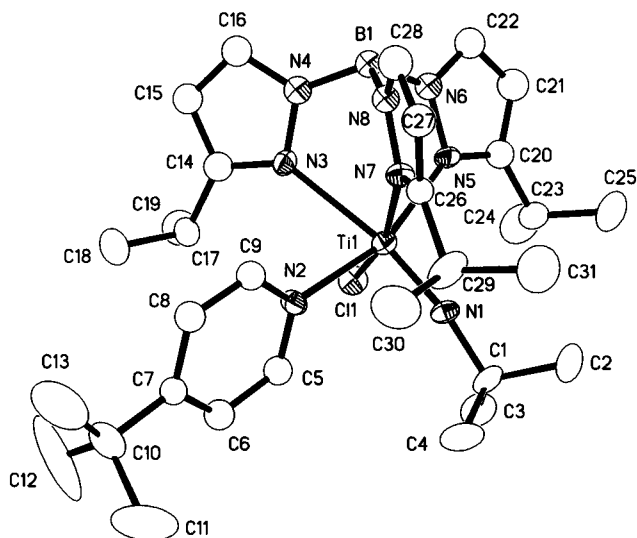
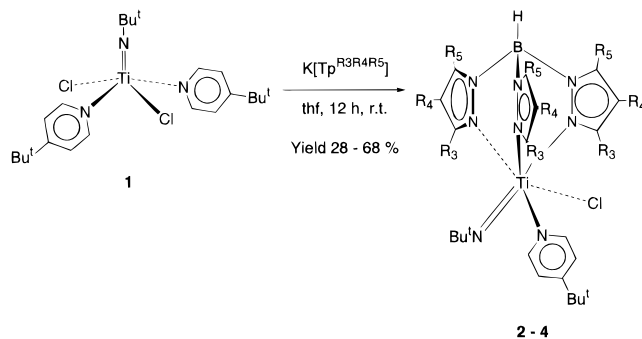


Figure 1. Molecular structure of [Tp^{Pri}Ti(NBu^t)Cl(py-Bu^t)] (**3**) viewed approximately perpendicular to the Ti(1)···B(1) vector. Hydrogen atoms were omitted for clarity.

Scheme 1. Synthesis of Imidotitanium Tris(pyrazolyl)hydroborates



Tp ^{R3R4R5}	Tp ^{Me2} (2)	Tp ^{Pri} (3)	Tp ^{Pri,Br} (4)
R ₃	Me	Pr ⁱ	Pr ⁱ
R ₄	H	H	Br
R ₅	Me	H	H

described in this report to use the 4-*tert*-butylpyridine co-ligand, and not pyridine itself or any other less effective base. Thus reaction of [Ti(NBu^t)Cl₂(py)₃]⁷ or [Ti(NBu^t)Cl₂(OPPh₃)₂]²¹ with K[Tp^{Me2}] gave impure products, the main component of which appeared to be [Tp^{Me2}Ti(NBu^t)Cl(3,5-dimethylpyrazole)] as indicated by ¹H NMR spectroscopy.⁷

X-ray Crystallographic Studies. The molecular structure of [Tp^{Pri}Ti(NBu^t)Cl(py-Bu^t)] (**3**) is shown in Figure 1. The X-ray structure confirms the expected κ^3 -coordination mode of the Tp^{Pri} ligand in **3**. Thus the titanium center is six-coordinate with three *fac*-sites being occupied by the Tp^{Pri} group and the remainder of the coordination sphere being completed by Cl, NBu^t, and py-Bu^t ligands.

The Ti=NBu^t bond length in **3** [Ti(1)–N(1) = 1.708(6) Å] is very close to that found in the related η -C₅Me₅ complex [(η -C₅Me₅)Ti(NBu^t)Cl(py)] [Ti=NBu^t = 1.696(4) and 1.698(4) Å; two molecules are in the asymmetric unit].¹⁸ The Ti=NBu^t bond length in **3** may also be compared with those found in the six-coordinate complexes [Ti(NBu^t)Cl₂(py)₃] [Ti=NBu^t = 1.696(4) and 1.706(4) Å; two molecules in the asymmetric unit],

(15) Sheldrick, G. M.; *Acta Crystallogr. Sect. A* **1990**, *46*, 467.

(16) Sheldrick, G. M. SHELXL-93. Institut für Anorganische Chemie der Universität Göttingen, Germany, 1993.

(17) Kouba, J. K.; Wreford, S. S. *Inorg. Chem.* **1976**, *15*, 2313.

(18) Bai, Y.; Noltemeyer, M.; Roesky, H. W. *Z. Naturforsch.* **1991**, *46B*, 1357.

(19) Hughes, D. L.; Leigh, G. J.; Walker, D. G. *J. Chem. Soc., Dalton Trans.* **1988**, 1153.

(20) Reger, D. L.; Tarquini, M. E.; Lebioda, L. *Organometallics* **1983**, *2*, 1763.

(21) Lewkebandra, T. S.; Sheridan, P. H.; Heeg, M. J.; Rheingold, A. L.; Winter, C. H. *Inorg. Chem.* **1994**, *33*, 5879.

and *fac*-[Ti(NBu^t)Cl₂(pmdeta)] [pmdeta = *N,N,N',N'',N'''*-pentamethyldiethylenetriamine; Ti=Nbu^t = 1.691(3) and 1.696(3) Å; two molecules are in the asymmetric unit].⁷ The Ti=N—Bu^t bond angle [Ti(1)—N(1)—C(1) = 169.6(6)°] is sufficiently close to linearity to suggest that the NBu^t ligand is able to act as a formal four-electron donor (taking NBu^t as a neutral ligand for electron-counting purposes) to the titanium center.^{1,2}

There is evidence for a strong structural influence of the NBu^t ligand in **3**. Thus the bond angles between the nitrogen atom [N(1)] of the NBu^t ligand and those atoms *cis* to it [Cl(1), N(2), N(5), N(7)] all exceed the 90° angle anticipated for ideal octahedral coordination, with the consequence that the Ti atom in **3** is displaced by 0.31 Å from the least-squares plane containing the atoms Cl(1), N(2), N(5), and N(7). The bond length between titanium and the nitrogen atom [N(3)] of the 3-isopropylpyrazole ring *trans* to the NBu^t group [Ti(1)—N(3) = 2.417(6) Å] is considerably longer than any of the distances between titanium and the nitrogen atoms of the *cis*-3-isopropylpyrazole or py-Bu^t moieties [Ti(1)—N(5) = 2.176(7), Ti(1)—N(7) = 2.208(6), Ti(1)—N(2) = 2.221(6) Å]. Such structural features in five- or six-coordinate complexes containing a metal—ligand multiple bond (such as imido, oxo or nitrido) are well-known and have been rationalized in terms of a combination of both electronic and steric effects.^{1,22} Similar structural effects have been found for related imido- and oxo-transition metal tris(pyrazolyl)hydroborato complexes.^{8,10,23} Interestingly in **3**, the lengthening of the bond between titanium and the 2-nitrogen [N(3)] of the pyrazole ring *trans* to NBu^t is accompanied by tighter binding of the 1-nitrogen to boron [N(4)—B(1) = 1.485(11) compared with N(6)—B(1) = 1.532(11) and N(8)—B(1) = 1.528(11) Å for the two “normal” pyrazole rings].

The titanium center in [Tp^{Pri}Ti(NBu^t)Cl(py-Bu^t)] (**3**) is clearly sterically crowded (as is also evident *inter alia* from the solution NMR spectra). The methyl groups of the 3-isopropyl substituents are all directed away from the metal center, while the ring nitrogen and carbon atoms of the py-Bu^t ligand are “sandwiched” between two 3-isopropyl pyrazole rings [those containing N(3) and N(4) and N(7) and N(8)] of the Tp^{Pri} ligand. The py-Bu^t ligand in **3** is, within *ca.* 20°, coplanar with the ring nitrogen and carbon atoms [N(5), N(6), C(20)—C(22)] of the 3-isopropylpyrazole ligand *trans* to it. As expected^{11,12} the atoms of the B—N—N—Ti—N—N—B metallocycles have an irregular boat conformation, and B(1) has an almost ideal tetrahedral geometry.

NMR Spectroscopic Studies. Room temperature and low temperature ¹H and ¹³C NMR spectra have been recorded for the three complexes [Tp^{Me2}Ti(NBu^t)Cl(py-Bu^t)] (**2**), [Tp^{Pri}Ti(NBu^t)Cl(py-Bu^t)] (**3**), and [Tp^{Pri,Br}Ti(NBu^t)Cl(py-Bu^t)] (**4**). Comparison of the low temperature NMR data for **3** with the solid-state X-ray structure suggests that this structure is maintained in solution. The similarity of the NMR (and IR) spectra of **2** and **4** to those of **3** are consistent with these complexes having structures analogous to that of **3**. For ease of interpretation, we shall discuss here only the NMR spectra of **2** in detail. The NMR spectra and dynamic behavior (*vide infra*) of **2**, **3**, and **4** are all very similar.

The 500 MHz ¹H NMR spectra of **2** in CD₂Cl₂ at 223 K and 298 K are shown in parts a and b of Figure 2, respectively. The

chemical shift assignments for **2** are from phase-sensitive NOESY DQF, selective ¹H decoupled homo- and heteronuclear, ¹³C{¹H} CPD, ¹³C{¹H} DEPT, and ¹H—¹³C correlation spectra (all using standard Bruker software), and by comparisons of the NMR spectra of **2**, **3**, and **4**. The 3,5-dimethyl pyrazole ring *trans* to NBu^t is taken as ring “number 1”, the ring *trans* to Cl as “number 2” and the remaining ring (*trans* to py-Bu^t) as “number 3”. The pyrazole methyls oriented toward the {Ti(NBu^t)Cl(py-Bu^t)} fragment are referred to as “d” (i.e. “down”, e.g. Me_{1d}) and those oriented toward the BH group as “u” (“up”, e.g. Me_{2u}). The py-Bu^t *ortho*-protons and -carbons are labeled “od” and “ou”, and the *meta*-protons and -carbons are labeled “md” and “mu”. The “u” (“up”) atoms are oriented toward the pyrazole rings and those labeled “d” (“down”) point away.

The complexes **2–4** are fluxional at room temperature. For example, it is immediately clear from parts a and b of Figure 2 that for **2** the resonances assignable to the ¹H atoms of the {Tp^{Me2}Ti(NBu^t)} fragment are essentially temperature independent, while the pyridine *ortho*- and *meta*-proton resonances show evidence of dynamic behavior for the py-Bu^t ligand. Thus in the 223 K ¹H NMR spectrum of **2** in CD₂Cl₂ (Figure 2a) four independent resonances for H_{mu}, H_{md}, H_{od}, and H_{ou} are observed, whereas at 298 K (Figure 2b) these resonances are very broad. In the 223 K ¹³C{¹H} NMR spectrum of **2** in CD₂Cl₂ (not illustrated) separate signals for the C_{mu}, C_{md}, C_{od}, and C_{ou} atoms are seen, but by 303 K C_{mu} and C_{md} have coalesced to give a single resonance and C_{od} and C_{ou} have broadened into the baseline (these resonances have a larger frequency separation in the slow exchange limit and thus a higher temperature would be required to achieve a fast-exchange regime²⁴). The NMR spectra are consistent with restricted rotation of the *tert*-butyl pyridine ligand, this process being “frozen out” on the NMR time scale at low temperature. Spin-saturation transfer (SST) ¹H NMR spectra confirm exchange between the H_{od} and H_{ou} sites.

We were intrigued by the apparently anomalous, high-field shift of the *ortho* proton resonance H_{ou}. The phase-sensitive ¹H NOESY DQF spectrum of **2** at 193 K suggests that the H_{ou} proton is close to the Me_{1d} and Me_{2d} groups and thus corresponds to the proton which, in **3**, would be attached to the py-Bu^t *ortho*-carbon C(9) (Figure 1). Therefore H_{ou} must be “sandwiched” between the 3,5-dimethyl pyrazole rings referred to above as “number 1” and “number 2” and so the high field shift reflects ring-current effects from the pyrazole rings. The compounds **3** and **4** also show high field shifts for this *ortho* hydrogen atom.

To rule out the possibility that an *ortho*-agostic²⁵ interaction in solution (albeit unlikely from the X-ray structure of **3**) gives rise to the high-field H_{ou} shifts in these formally 16-electron complexes, we measured the individual *ortho* C—H coupling constants for **2**, **3** and **4** in the low temperature 223 K limit (where *k*_{exch} < 5 s⁻¹ ≪ ¹J[C_{od}—H_{od}] or ¹J[C_{ou}—H_{ou}]). The values for ¹J[C_{od}—H_{od}] and ¹J[C_{ou}—H_{ou}] are 183 and 183 (**2**), 184 and 183 (**3**), and 182 and 181 Hz (**4**), respectively. These magnitudes can be compared to values (in CD₂Cl₂) of ¹J[C_{ortho}—H] for free py-Bu^t (177 Hz) and for the pyridine ligand in the related valence isoelectronic complex [(η-C₅Me₅)Ti(NBu^t)Cl(py-Bu^t)] (179 Hz).⁶ The η-pentamethylcyclopentadienyl complex does not show evidence for restricted *tert*-butylpyridine rotation down to 213 K. The ¹J[C_{od}—H_{od}] and ¹J[C_{ou}—H_{ou}] coupling constants for **2–4** are equivalent within experimental

(22) Lyne, P. D.; Mingos, D. M. P. *J. Chem. Soc., Dalton Trans.* **1995**, 1635.

(23) Roberts, S. A.; Young, C. G.; Kipke, C. A.; Cleland, W. E.; Yamanouchi, K.; Carducci, M. D.; Enemark, J. H. *Inorg. Chem.* **1990**, *29*, 3650.

(24) Sandström, J. *Dynamic NMR Spectroscopy*; Academic Press: London, 1992.

(25) Brookhart, M.; Green, M. L. H.; Wong, L.-L. *Prog. Inorg. Chem.* **1988**, *36*, 1.

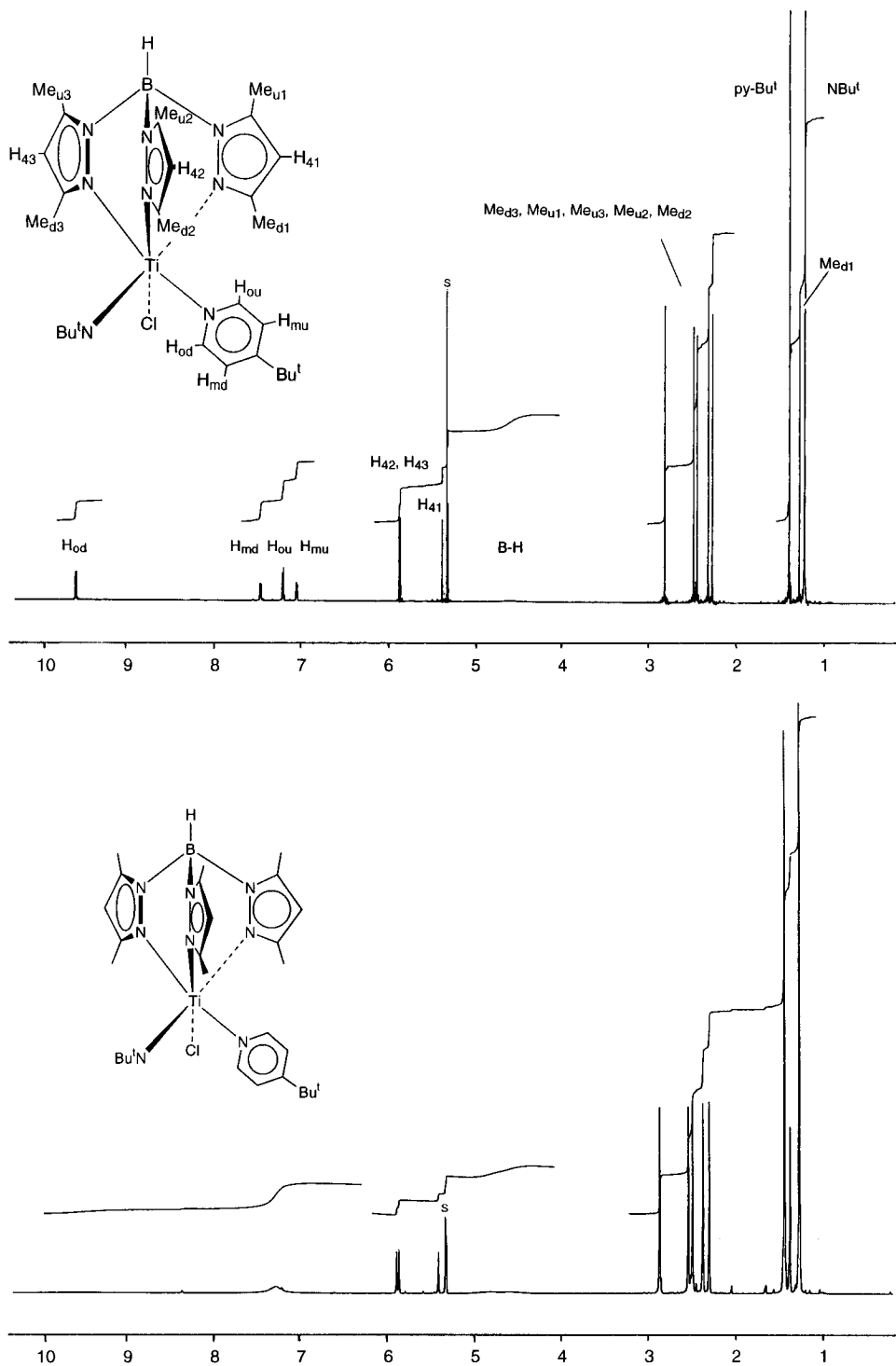


Figure 2. 500 MHz ^1H NMR spectra of $[\text{Tp}^{\text{Me}_2}\text{Ti}(\text{NBu})\text{Cl}(\text{py-Bu})]$ (**2**) at 223 (a, upper) and 298 K (b, lower) in CD_2Cl_2 . Residual protio solvent peak indicated by "s". No particular bond order is implied by the wedged line connecting the Ti and imido N atom which is used only to indicate the relative geometry.

error and are, in fact, slightly greater than the corresponding values for free py-Bu^t and $[(\eta\text{-C}_5\text{Me}_5)\text{Ti}(\text{NBu})\text{Cl}(\text{py-Bu})]$. For comparison, the 16-electron cation $[(\eta\text{-C}_5\text{Me}_5)_2\text{Zr}(\text{Me})(2\text{-py-Me})]^+$ (2-py-Me = 2-methylpyridine) does have an *ortho*-agostic bond which is revealed by a significantly reduced $^1J[\text{C}_{\text{ortho}}\text{-H}]$ value of 168 Hz.²⁶ We thus conclude that restricted pyridine rotation in **2–4** and the high-field shift of H_{ou} are due to steric hinderance and subsequent anisotropic shielding effects. Interestingly, the molybdenum oxo complex $[\text{Tp}^{\text{Me}_2}\text{Mo}(\text{O})\text{Cl}$

(py)], first reported by Enemark,²³ shows *five* pyridine proton resonances at room temperature, indicating that pyridine rotation in this complex is frozen out on the 400 MHz ^1H NMR time scale.²⁷

Finally it is noteworthy that the methyl group and the ring CH resonances ($\text{Me}_{\text{u}1}$, $\text{Me}_{\text{d}1}$, and H_{41} , respectively) for the pyrazolyl ring *trans* to NBu^t are the most shielded of the sets of resonances $\text{Me}_{\text{u}(1-3)}$, $\text{Me}_{\text{d}(1-3)}$, and $\text{H}_{4(1-3)}$. This is probably due the *trans* influence of the NBu^t ligand, rather than to shielding effects of neighboring groups since we have already

(26) Jordan, R. F.; Taylor, D. F.; Baenziger, N. C. *Organometallics* **1990**, *9*, 1546.

(27) Sundermeyer, J. Personal communication.

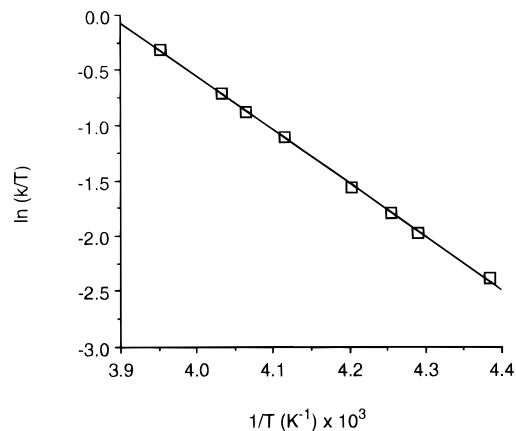


Figure 3. Eyring plot for pyridine rotation in $[\text{Tp}^{\text{Me}_2}\text{Ti}(\text{NBu}^t)\text{Cl}(\text{py-Bu}^t)]$ (**2**). Refer to the text and Table 3 for further details.

Table 3. Rate Constants and Derived Activation Parameters for Pyridine Rotation in $[\text{Tp}^{\text{Me}_2}\text{Ti}(\text{NBu}^t)\text{Cl}(\text{py-Bu}^t)]$ (**2**)

(i) From ^{13}C Line Shape Analysis (See Text for Details)			
temp (K)	av cor $\nu_{1/2}$ (Hz)	k_{obs} (s^{-1})	k_{exch} (s^{-1})
228	3.3	10.4	20.8
233	5.2	16.3	32.6
235	6.2	19.5	39.0
238	7.9	24.8	49.6
243	12.8	40.2	80.4
246	16.2	50.9	102
248	19.7	61.9	124
253	29.3	92.1	184

$$\Delta H^\ddagger = 40.2 \text{ kJ mol}^{-1}; \Delta S^\ddagger = -42.0 \text{ J mol}^{-1} \text{ K}^{-1};$$

$$\Delta G^\ddagger_{267 \text{ K}} = 51.4 \text{ kJ mol}^{-1}$$

(ii) From ^{13}C Coalescence of C_{mu} and C_{md} at 267 K (See Text for Details)

$$k_{\text{chem}} = 564 \text{ s}^{-1}$$

$$\Delta G^\ddagger_{267 \text{ K}} = 51.1 \text{ kJ mol}^{-1}$$

established from the X-ray structure of **3** that the pyrazole ring *trans* to NBu^t is relatively weakly coordinated and thus would be expected to carry a greater build-up of electron density.

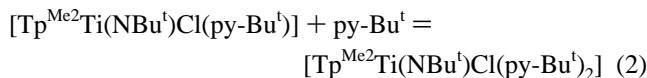
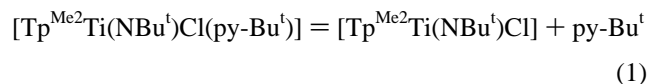
Activation parameters for pyridine rotation in $[\text{Tp}^{\text{Me}_2}\text{Ti}(\text{NBu}^t)\text{Cl}(\text{py-Bu}^t)]$ (**2**) were obtained from $^{13}\text{C}\{^1\text{H}\}$ NMR spectra of **2** between $228 \leq T \leq 253$ K in the slow exchange regime. Curve fitting (standard Bruker software) of the pyridine *ortho*- and *meta*- carbon resonances afforded $\nu_{1/2}$ (band width at half-height) values from which were subtracted the natural line widths as obtained at 203 K to give corrected $\nu_{1/2}$ values. At each temperature, the 1st-order k_{obs} value was calculated from the average corrected $\nu_{1/2}$ value (Table 3) according to the expression $k_{\text{obs}} = \pi\nu_{1/2}$. Taking chemical exchange rate constants (k_{exch}) as $2k_{\text{obs}}$ ^{24,28} we obtained the activation parameters listed in Table 3 from the Eyring plot shown in Figure 3. As a check of the reliability of the ΔS^\ddagger and ΔH^\ddagger values obtained from the lineshape analysis, we extracted $\Delta G^\ddagger_{267 \text{ K}}$ (Table 3) from $^{13}\text{C}\{^1\text{H}\}$ coalescence measurements for the py-Bu^t C_{mu} and C_{md} resonances (at 267 K) using standard procedures.²⁴ The value of $\Delta G^\ddagger_{267 \text{ K}}$ from coalescence measurements (51.1 kJ mol^{-1}) compares very well with the value of $\Delta G^\ddagger_{267 \text{ K}}$ (51.4 kJ mol^{-1}) calculated from the ΔS^\ddagger and ΔH^\ddagger values from ^{13}C lineshape analysis. The values obtained for ΔG^\ddagger are reasonable. For example, the barrier to pyridine rotation in $[(\eta\text{-C}_5\text{H}_7)_2\text{Nb}(\text{H})\text{(py)}]$ is reported to be $\Delta G^\ddagger_{258 \text{ K}} = 52 \pm 1 \text{ kJ mol}^{-1}$.²⁹

Table 4. $\Delta\delta$ values for $[\text{Ti}(\text{NBu}^t)\text{Cl}_2(\text{py-Bu}^t)_2]$ (**1**) and $[(\text{L})\text{Ti}(\text{NBu}^t)\text{Cl}(\text{py-Bu}^t)]$ [$\text{L} = \text{Tp}^{\text{Me}_2}$ (**2**), Tp^{Pri} (**3**), $\text{Tp}^{\text{Pri,Br}}$ (**4**), $\eta\text{-C}_5\text{H}_5$ (**5**) or $\eta\text{-C}_5\text{Me}_5$ (**6**)]^a

compd	C_α (ppm)	C_β (ppm)	$\Delta\delta$ (ppm) ^b	ref
$[\text{Ti}(\text{NBu}^t)\text{Cl}_2(\text{py-Bu}^t)_2]$ (1)	73.6	30.6	43.0	6, 7
$[(\text{Tp}^{\text{Pri,Br}})\text{Ti}(\text{NBu}^t)\text{Cl}(\text{py-Bu}^t)]$ (4)	71.1	30.4	40.7	This work
$[(\text{Tp}^{\text{Pri}})\text{Ti}(\text{NBu}^t)\text{Cl}(\text{py-Bu}^t)]$ (3)	70.2	30.8	39.4	This work
$[(\text{Tp}^{\text{Me}_2})\text{Ti}(\text{NBu}^t)\text{Cl}(\text{py-Bu}^t)]$ (2)	69.5	31.2	38.4	This work
$[(\eta\text{-C}_5\text{H}_5)\text{Ti}(\text{NBu}^t)\text{Cl}(\text{py-Bu}^t)]$ (5)	69.0	31.5	37.5	6, 30
$[(\eta\text{-C}_5\text{Me}_5)\text{Ti}(\text{NBu}^t)\text{Cl}(\text{py-Bu}^t)]$ (6)	68.9	32.2	36.7	6, 30

^a All values in CDCl_3 at 298 K. ^b $\Delta\delta = \delta(\text{C}_\alpha) - \delta(\text{C}_\beta)$ (see text for details).

The small, negative ΔS^\ddagger ($-48 \text{ J mol}^{-1} \text{ K}^{-1}$) is consistent with an ordering in the transition state associated with the exchange process in **2**. It would also appear to eliminate an exchange mechanism of the type described by eq 1, where dissociation



of the coordinated py-Bu^t ligand occurs prior to scrambling of magnetisation. In addition, the five-coordinate $[\text{Tp}^{\text{Me}_2}\text{Ti}(\text{NBu}^t)\text{Cl}]$ intermediate formed in such a dissociative mechanism would be expected to collapse to C_s symmetry, with the consequence that the sets of resonances for two of the Tp^{Me_2} 3,5-dimethylpyrazole rings should show evidence of pairwise exchange in the NMR spectra of **2**. Furthermore, we have found that “free” py-Bu^t added to an ^1H NMR sample of **2** does not undergo exchange with coordinated py-Bu^t on the NMR time scale, as would normally be expected from the process described by eq 1. This NMR tube experiment also rules out an associative py-Bu^t exchange mechanism—on the NMR time scale—(eq 2) of the type that we have shown to occur in the related half-sandwich η -cyclopentadienylimidotitanium complexes $[(\eta\text{-C}_5\text{Me}_4\text{R})\text{Ti}(\text{NBu}^t)\text{Cl}(\text{py-R}')] (R = \text{Me, Et or } \text{CH}_2\text{-CH}_2\text{CHCH}_2; \text{py-R}' = \text{py-Bu}^t \text{ or py})$.³⁰

Evaluation of L-Group Donor Ability in the Imidotitanium Complexes $[(\text{L})\text{Ti}(\text{NBu}^t)\text{Cl}(\text{py-Bu}^t)]$ ($\text{L} = \eta\text{-C}_5\text{H}_5, \eta\text{-C}_5\text{Me}_5, \text{Tp}^{\text{Me}_2}, \text{Tp}^{\text{Pri}}, \text{ or } \text{Tp}^{\text{Pri,Br}}$). The complexes **2–4**, together with their η -cyclopentadienyl analogues $[(\eta\text{-C}_5\text{R}_5)\text{Ti}(\text{NBu}^t)\text{Cl}(\text{py-Bu}^t)] [R = \text{H} (\mathbf{5}) \text{ or } \text{Me} (\mathbf{6})]$ ⁶ offer the possibility of investigating the relative donor abilities of the various tris(pyrazolyl)hydroborate and cyclopentadienyl ligands in (*tert*-butylimido)titanium complexes. For *tert*-butyl imido groups, the difference ($\Delta\delta$) between the ^{13}C NMR chemical shifts (δ) of the so-called “ C_α ” ($=\text{NCMe}_3$) and “ C_β ” ($=\text{NCMe}_3$) atoms can give an indication of the electron density at the imido nitrogen atom.³¹ Large $\Delta\delta$ values are associated with electrophilic nitrogen atoms and small Δ values with nucleophilic behavior of the imido nitrogen. The $\Delta\delta$ -values ($\Delta\delta = \delta(\text{C}_\alpha) - \delta(\text{C}_\beta)$) for the compounds **2–6** are listed in Table 4, together with the $\Delta\delta$ -value for $[\text{Ti}(\text{NBu}^t)\text{Cl}_2(\text{py-Bu}^t)_2]$ (**1**) for comparison.

The data in Table 4 suggest that the imido nitrogen atoms in the cyclopentadienyl complexes **5–6** are more nucleophilic than those in the tris(pyrazolyl)hydroborates **2–4** and that the imido

(28) Green, M. L. H.; Wong, L.-L.; Sella, A. *Organometallics* **1992**, *11*, 2660.

(29) Green, M. L. H.; Hughes, A. K. *J. Chem. Soc., Dalton Trans.* **1992**, 527.

(30) Butakoff, K. A.; Dunn, S. C.; Mountford, P.; Robson, D. A. Manuscript in preparation.

(31) Nugent, W. A.; McKinney, R. J.; Kasowski, R. V.; Van-Catledge, F. A. *Inorg. Chim. Acta* **1992**, *65*, L91.

nitrogen atom in the 14-electron **1** is the least nucleophilic for the six complexes listed. The apparent build up of electron density on the imido N on passing from **5** to **6** correlates with the increased donor ability of $\eta\text{-C}_5\text{Me}_5$ compared to $\eta\text{-C}_5\text{H}_5$. For the series **2–4** there is a gradual increase in $\Delta\delta$ which presumably reflects a decrease in donor ability of the pyrazole rings on going from a 3,5-dimethyl-, to a 3-isopropyl-, to a 3-isopropyl-4-bromo-substituted system. The trend in $\Delta\delta$ values for **2–4** is also maintained in CD_2Cl_2 solution (**2**, $\Delta\delta = 38.7$; **3**, $\Delta\delta = 39.8$; **4**, $\Delta\delta = 41.0$ ppm; $\Delta\delta$ values at 298 and at 223 K are identical within error).

It is interesting to compare this measure of donor ability of various cyclopentadienyl and tris(pyrazolyl)hydroborate groups with more conventional approaches such as measuring IR frequencies of other functional groups present. Thus $\nu(\text{CO})$ (a' and a'' mode) values have been reported for the complexes $[(\text{L})\text{Rh}(\text{CO})_2]$ where $\text{L} = \eta\text{-C}_5\text{Me}_5$ [average $\nu(\text{CO}) = 1993.0 \text{ cm}^{-1}$ (hexane)],³² $\eta\text{-C}_5\text{H}_5$ [average $\nu(\text{CO}) = 2015.5 \text{ cm}^{-1}$ (hexane)],³² $\kappa^3\text{-Tp}^{\text{Me}2}$ [average $\nu(\text{CO}) = 2017.5 \text{ cm}^{-1}$ (hexane)]³³ or 2013 cm^{-1} (KBr)³⁴ or $\kappa^3\text{-Tp}^{\text{Me}}$ [$\text{Tp}^{\text{Me}} = \text{tris}(3\text{-methylpyrazolyl})\text{-hydroborate}$]; average $\nu(\text{CO}) = 2021 \text{ cm}^{-1}$ (KBr)].³⁴ Unfortunately the $\{\text{Rh}(\text{CO})_2\}$ derivative of $\text{Tp}^{\text{Pri,Br}}$ has the tris(3-isopropyl-4-bromopyrazolyl)hydroborate ligand in a κ^2 coordination mode,³⁴ and the Tp^{Pri} derivative has not yet been reported. In a related study, Sundermeyer has reported the IR spectra of $[(\text{L})\text{M}(\text{O})_2\text{R}]$ ($\text{L} = \eta\text{-C}_5\text{Me}_5$ or $\text{Tp}^{\text{Me}2}$; $\text{M} = \text{Mo}$ or W ; $\text{R} = \text{Me}$ or CH_2SiMe_3).³⁵ In these complexes $\nu_{\text{sym}}(\text{M}=\text{O})$ and $\nu_{\text{asym}}(\text{M}=\text{O})$ are, without exception, higher in frequency for the weaker donor $\text{Tp}^{\text{Me}2}$ ligand.

From the $\Delta\delta$ values for the series $[(\text{L})\text{Ti}(\text{NBu}^t)\text{Cl}(\text{py-Bu}^t)]$ (**2–6**), we propose that the donor ability of the L ligands increases in the order $\text{Tp}^{\text{Pri,Br}} < \text{Tp}^{\text{Pri}} < \text{Tp}^{\text{Me}2} < \eta\text{-C}_5\text{H}_5 < \eta\text{-C}_5\text{Me}_5$. For the series $[(\text{L})\text{Rh}(\text{CO})_2]$ where one uses average $\nu(\text{CO})$ values as an indicator of electron density at the metal center, the series is best described as $\text{Tp}^{\text{Me}} < \text{Tp}^{\text{Me}2} \approx \eta\text{-C}_5\text{H}_5 < \eta\text{-C}_5\text{Me}_5$ (a truly rigorous comparison, however, cannot be made since IR data for the entire rhodium series in the same medium are not currently available). For the compounds $[(\text{L})\text{M}(\text{O})_2\text{R}]$ it is found that the donor ability of $\text{Tp}^{\text{Me}2} < \eta\text{-C}_5\text{Me}_5$. If we assume that the inductive effect of Me (in Tp^{Me}) is very similar to that of Pr^i (in Tp^{Pri}) then it appears that $\Delta\delta$ values give essentially the same ordering of donor ability of the

cyclopentadienyl and tris(pyrazolyl)hydroborate ligands as “conventional” $\nu(\text{CO})$ or $\nu(\text{M}=\text{O})$ values. The influence of variable local magnetic anisotropy of the different L-ligands on the $\Delta\delta$ values is probably therefore not significant in the complexes under study here.

Curtis and co-workers have suggested that Tp is a slightly better donor than $\eta\text{-C}_5\text{H}_5$ based on Mulliken population analyses obtained from EHMO calculations on $[\text{TpMo}(\text{CO})_3]$ and $[(\eta\text{-C}_5\text{H}_5)\text{Mo}(\text{CO})_3]$.³⁶ Such analyses are very basis-set dependent, and it is possible that relatively small changes in the energies of the donor/acceptor orbitals in question could lead to a reversal of the predicted donor abilities of these two groups.³⁷

Summary and Conclusions

(*tert*-Butylimido)titanium complexes containing a tris(pyrazolyl)hydroborate co-ligand are readily prepared from $[\text{Ti}(\text{NBu}^t)\text{Cl}_2(\text{py-Bu}^t)_2]$ and the potassium salt of the appropriate tris(pyrazolyl)hydroborate. The X-ray structure of **3** has been determined and the NMR spectra of **2–4** are consistent with six-coordinate, κ^3 -tris(substituted-pyrazolyl)hydroborate structures in solution. The complexes are fluxional and activation parameters for *tert*-butylpyridine rotation in **2** have been determined. ^{13}C NMR $\Delta\delta$ values ($\Delta\delta = \delta(\text{C}_\alpha) - \delta(\text{C}_\beta)$) for the imido *tert*-butyl groups in **2–4**, both in CDCl_3 and in $\text{CD}_2\text{-Cl}_2$, indicate that while the donor ability of the tris(pyrazolyl)hydroborate ligands increases in the order $\text{Tp}^{\text{Pri,Br}} < \text{Tp}^{\text{Pri}} < \text{Tp}^{\text{Me}2}$, these ligands are not as effective donors to the metal center as either $\eta\text{-C}_5\text{H}_5$ or $\eta\text{-C}_5\text{Me}_5$.

Acknowledgment. We thank the EPSRC (studentship to S.C.D.) and the University of Nottingham (New Lecturer’s Research Grant, NLRG 049) for support, Drs. D. Pert (Bruker) and A. G. Avent (University of Sussex) for the low temperature ^1H NOESY DQF and 500 MHz ^1H NMR spectra respectively, Mr. K. A. Butakoff for providing samples of $\text{K}[\text{Tp}^{\text{Pri}}]$ and $\text{K}[\text{Tp}^{\text{Pri,Br}}]$, and Dr. A. J. Blake and a referee for helpful comments.

Supporting Information Available: Tables of crystal data and structure refinement procedures, complete bond lengths and angles, anisotropic displacement parameters, hydrogen atom coordinates, isotropic and equivalent isotropic displacement parameters and an alternative view of the structure of **3** (8 pages). Ordering information is given on any current masthead page.

IC9510674

(32) Kakkar, A. K.; Taylor, N. J.; Marder, T. B.; Shen, J. K.; Hallinan, N.; Basolo, F. *Inorg. Chim. Acta* **1992**, 198–200, 219.

(33) Ghosh, C. K.; Graham, W. A. G. *J. Am. Chem. Soc.* **1987**, 109, 4727.

(34) Bucher, U. E.; Currao, A.; Nesper, R.; Rüegger, H.; Venanzi, L. M.; Younger, E. *Inorg. Chem.* **1995**, 34, 66.

(35) Sundermeyer, J.; Putterlik, J.; Pritzkow, H.; *Chem. Ber.* **1993**, 126, 289.

(36) Curtis, M. D.; Shiu, K.-B.; Butler, W. M.; Huffman, M. D.; *J. Am. Chem. Soc.* **1986**, 108, 3335.

(37) Albright, T. A.; Burdett, J. K.; Whangbo, M.-H. *Orbital Interactions in Chemistry*; Wiley-Interscience: New York, 1985.